Biophysical Chemistry 168–169 (2012) 48–59

Contents lists available at SciVerse ScienceDirect

Biophysical Chemistry

journal homepage: http://www.elsevier.com/locate/biophyschem

Modulation of the neurotensin solution structure in the presence of ganglioside GM1 bicelle

Ummul Liha Khatun [a], Sudipto Kishore Goswami [b], Chaitali Mukhopadhyay [a,*]

[a] Department of Chemistry, University of Calcutta, 92, A.P.C Road, Kolkata 700009, India
[b] NMR Application Chemist, Bruker India Scientific Private Limited, 22 B Ruby Park South, Kolkata 700078, India

HIGHLIGHTS

- ► NT is predominantly unstructured in aqueous solution.
- ► In the presence of PC bicelle NT adopts 3_{10} helical structure.
- ► In GM1 bicelle NT adopts predominating 3_{10} helical structure.
- ► Small fraction of α-helical structure also acquired in GM1 bicelle.
- ► NT interacts strongly with GM1 bicelle than that of the PC bicelle.

GRAPHICAL ABSTRACT

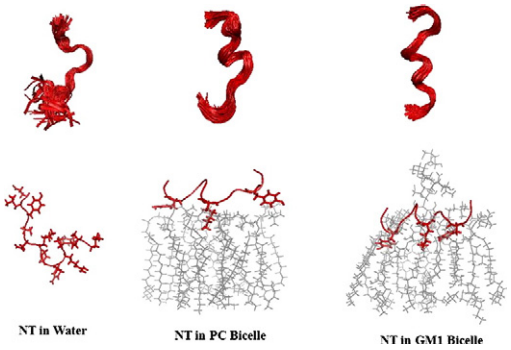

ARTICLE INFO

Article history:
Received 18 April 2012
Received in revised form 25 June 2012
Accepted 26 June 2012
Available online 2 July 2012

Keywords:
Neurotensin
GM1
Bicelle
NMR
NTS3
Docking

ABSTRACT

Neurotensin (NT) is an endogenous tridecapeptide neurotransmitter that shows multiple biological function in central and peripheral nervous systems. Gangliosides are glycosphingolipids, most abundant in the plasma membrane of nerve cells. Here we investigate the change of neurotensin solution structure induced by isotropic CHAPS-PC bicelles with and without ganglioside GM1 using solution state NMR spectroscopy. In aqueous solution the peptide is predominately unstructured. In the presence of bicelle overall structure of the peptide is stabilized. In CHAPS-PC bicelle neurotensin adopts 3_{10} helical structure. In the presence of GM1 containing bicelle, the peptide adopts predominately 3_{10} helical structures with small amount of α-helical structure. These results are consistent with the CD spectroscopic results. Neurotensin interacts better with GM1 containing bicelle than that of the CHAPS-PC bicelle. Docking studies between the Neurotensin Receptor3 (NTS3) and different NT conformations also indicated better binding of the NT conformation obtained in presence of GM1-containing bicelles.

Abbreviations: NT, Neurotensin; GM1, Ganglioside Monosialo 1; DMPC, 1, 2- dimyristoyl-sn-glycero-3-phosphatidylcholine; CHAPS, 3-[(3-Cholamidopropyl) dimethylammonio]-1-propanesulfonate; DHPC, 1, 2- dihexanoyl-sn-glycero-3-phosphocholine; DPC, Dodecylphosphocholine; HFIP, Hexafluoroisopropanol; TFE, Tetrafluoroethylene; DMPG, 1, 2-dimyristoyl-*sn*-glycero-3-[phospho-rac-(1-glycerol)]; SDS, Sodium dodecyl sulfate; NMR, Nuclear Magnetic Resonance; TOCSY, Total Correlation Spectroscopy; ROESY, Rotating-frame Overhauser Effect Spectroscopy; NOESY, Nuclear Overhauser Effect Spectroscopy; DQF- COSY, Double Quantum Filtered-Correlation Spectroscopy; ROE, Rotating-frame NOE; DOSY, Diffusion Ordered Spectroscopy; CD, Circular Dichroism; NTS3, Neurotensin Receptor3; ADT, Auto Dock Tools.

* Corresponding author. Tel.: +91 33 2351 8386; fax: +91 33 2351 9755.
E-mail addresses: chaitalicu@yahoo.com, cmchem@caluniv.ac.in (C. Mukhopadhyay).

0301-4622/$ – see front matter © 2012 Elsevier B.V. All rights reserved.
doi:10.1016/j.bpc.2012.06.003

1. Introduction

Neurotensin, a tridecapeptide, was first isolated from the bovine hypothalamus [1,2]. It is distributed throughout the central as well as peripheral nervous systems and in the gastrointestinal system of various animals including birds [3]. NT is also widely distributed throughout the mammalian brain [3]. It shows diverse biological activity. In peripheral nervous system, NT acts as the paracrine and endocrine modulator of the digestive tract [4] while in the central nervous system NT shows antinociception, hypothermia and increased locomotors activity [5]. These processes are reported to be mediated through the regulation of the mesolimbic and negrostriatal dopamine pathways [5]. Hence neurotensin has similar pharmacological action as that of dopamine which act as antipsychotics [5]. Therefore, NT can be used as the target in the treatment of neurodegenerative diseases [6]. Neurotensin promote the cancer growth [7] whereas neurotensin agonist and antagonist are used in the treatment of pain as painkiller, eating disorders, psychiatric disorders, substance abuse , stress and inhibit tumor/cancer growth [8,9].

The relevance of studying a water soluble neurotransmitter neurotensin in a membrane mimetic environment is that activities of NT are related to its binding to different transmembrane receptors with various affinities [10]. Biologically active peptides bind first to the membrane in a non specific manner, and then migrate and bind specifically to their receptors by lateral diffusion on the membrane surface [10]. Therefore, it is necessary to investigate the interaction of neurotensin with membrane and to characterize the membrane bound conformation which in turn might control the receptor binding and subtype selectivity. Despite the clinical importance of this peptide, very little is known regarding the structure of NT in its membrane bound form. Xu et al. studied the structure of full length NT in presence of Sodium dodecyl sulfate (SDS) micelle using solution state 2D-NMR spectroscopy and reported that three cationic C-terminal residues of NT bind with the anionic sulfate head group of micelles [11]. But complete information regarding the structure of neurotensin in presence of SDS micelle was lacking because of excessive line broadening of the ^{1}H NMR spectra [11]. Another study has been done by Coutant et al., on full length neurotensin in three membrane mimetic environments i.e., Dodecylphosphocholine(DPC) micelle, Tetrafluoroethylene (TFE) and Hexafluoroisopropanol (HFIP) [10]. Using solution state 2D-NMR spectroscopy they proposed that in DPC micelle the C-terminus of full length NT shows a bent structure close to a type-I turn from Pro10 to Leu13, suggesting that the hydrophobic side chains of the turn are involved in interactions with the micelles [10], while in TFE and HFIP, full-length NT has an extended though slightly bent structure [10]. The N-terminal part of full length NT was found to be similar in TFE and in DPC micelle showing an extended conformation, whereas it presented a turn in HFIP solvent [10]. It is suggested that the central region of NT remains highly flexible in three membrane-mimetic environments [10]. Thus it remains to be speculated whether the observed lack of structure of NT seems from the inherent flexibility of NT or it arises from the limitations of the membrane-mimetic environments chosen till date. We report here a study of the solution conformation of NT in presence of CHAPS-PC bicelles with or without ganglioside GM1.

Gangliosides are complex glycosphingolipids consisting of mono- to poly-sialylated oligosaccharide chains of variable lengths attached to a ceramide unit [12,13]. They are inserted in the outer layer of the plasma membrane with the hydrophobic ceramide moiety acting as an anchor while oligosaccharide moiety is exposed to the external medium [12,13]. Gangliosides are most abundant in the plasma membrane of nerve cells (10–12 mol% of the total lipid mass) [14] and are found widely in most vertebrate cell types [15]. Gangliosides help to maintain membrane structure and organization [16] and act as the receptor of lectins [17], toxins [18] and pathogens [19]. Gangliosides participate in a variety of cell surface events like cell-to-cell communication, cell matrix recognition [20].Within membrane micro domains, gangliosides act as modulators of cell signaling pathways, and interact with signal transducers [21]. The importance of gangliosides in human health is evident in neuro degenerative diseases such as Alzheimer's, Parkinson's, Huntington's disease, etc [22–24]. Tumor cells with a pharmacologically decreased concentration of gangliosides produce fewer tumors than do untreated cells, suggesting that pharmacologic depletion of gangliosides should be explored as a therapeutic approach to cancer [25]. In the present study we have used Ganglioside Monosialo 1(GM1) -doped fast tumbling isotropic ternary bicelle, composed of 1,2-dimyristoyl-sn-glycero-3-phosphocholine(DMPC),3-(cholamidopropyl)-dimethylammonio-2-hydroxyl-1-propane-sulfonate(CHAPS) and GM1 (1:4:0.3 mol ratio), as model membrane system for studying the effect of GM1 as a nerve cell membrane constituent on the conformation of neurotensin. To the best of our knowledge this is the first structural study of full length neurotensin in isotropic CHAPS-PC bicelle with or without ganglioside GM1 using solution state 2-D Nuclear Magnetic Resonance (NMR) spectroscopy.

2. Materials and methods

2.1. Materials

Neurotensin, DMPC(1,2-Dimyristoyl-sn-glycero-3-phosphosphatidylcholine), CHAPS [(3-cholamidopropyl)-dimethylammonio-2-hydroxyl-1-propane-sulfonate] and D_2O were purchased from Sigma Aldrich Pvt. Ltd.(USA) and used without further purification. GM1 was isolated and purified from goat brain in our laboratory following the published protocol [26]. Deionized water of pH 5.5 was used throughout the experiment to avoid salt interference on the binding of peptide to the negatively charge GM1 containing bicelle.

2.2. Bicelle preparation

Fast tumbling isotropic DMPC/CHAPS (1:4) and DMPC/CHAPS/GM1 (1:4:0.3) bicelle were prepared using our published protocol [27,28]. Briefly, to prepare DMPC/CHAPS bicelle appropriate amount of DMPC was weighted first and then suspended in deionized H_2O of pH 5.5. Hydrated samples were centrifuged, vigorously stirred in a vortex mixer and centrifuged again at room temperature until homogenous slurry was formed. Now appropriate amount of CHAPS from 400 mM stock solution (in deionized H_2O of pH 5.5) was added to the slurry so that q becomes 0.25 followed by vortexing until a clear and transparent solution was obtained.

Bicelle with negatively charged surfaces were produced by incorporating GM1 in the bicelle at 30 mol% of the phospholipid (DMPC). Appropriate amounts of DMPC and GM1 were weighted separately and then stocked together. Now GM1 and DMPC were suspended in deionized H_2O of pH 5.5 to prepare homogeneous slurry. Appropriate amount of CHAPS from 400 mM stock solution was added to the slurry to make the solution clear and transparent following the above stated protocol. Deionized water of pH 5.5 was used for bicelle preparation. The pH was adjusted by adding small volumes of 1M HCl or 1M NaOH. No buffer was used in order to keep the ionic strength minimum.

2.3. Fluorescence spectroscopy

The fluorescence experiments were performed using a Perkin-Elmer LS-50B spectrometer at the room temperature. An excitation wavelength of 275nm was used for all the experiments. Background intensities of the CHAPS-PC bicelle and the GM1 containing bicelle without neurotensin were subtracted from each neurotensin containing bicelle spectrum to discard any contribution from the solvent. The concentration of the peptide in solution was 150 μM and small aliquots from the 123 mM stock solution of the bicelle were added gradually to the peptide solution so that the concentration of the peptide remained unaltered in the medium.

2.4. CD spectropolarimetry

Far UV-CD spectra were acquired on a MOS-450 spectrometer using a silica quartz cell of 0.1 cm path length at room temperature. Records were averaged over 3 scans collected over the interval of 190 to 250 nm. Background spectra of deionized water (pH 5.5), DMPC/CHAPS and DMPC/CHAPS/GM1 bicelle solutions were used as control and were subtracted from each of the peptide spectra in water and in presence of bicelle. The respective intensities are expressed in terms of mean residue molar ellipticity $[\theta] = 100[\theta]_{obs}/CLn$, where $[\theta_{obs}]$ is the observed ellipticity in millidegrees, L is the optical path length in centimeter (0.1 cm in the present case), n is the number of amino acid residues and C is the molar concentration of the peptide. The peptide concentration was 1.5 mM and peptide: lipid mol ratio was 1:20.

2.5. NMR sample preparation

For NMR experiment concentration of the peptide used was 4.5 mM. 3.75 mg neurotensin (powder) was dissolved in the 500 μL of 90 mM each bicelle solution i.e., DMPC/CHAPS (1:4) and DMPC/CHAPS/GM1 (1:4:0.3) to maintain peptide: lipid mol ratio 1:20.

2.6. Collection and processing of solution NMR data

The NMR spectra were recorded on a Bruker DRX spectrometer equipped with a 5 mm broadband inverse probe head operating at a ^1H frequency of 500 MHz. All measurements were carried out at room temperature. 10% D_2O was added to lock the field frequency and all the spectra were referenced to the HDO peak at 4.782 ppm. Suppression of water signal was achieved using 3–9–19 pulse sequence with gradients. Two dimensional TOCSY (total correlation spectroscopy), ROESY (rotating frame overhauser effect spectroscopy) and DQF-COSY (double quantum filtered correlation spectroscopy) were collected in the phase sensitive mode. The TOCSY pulse sequence included 60 ms MLEV17-spin lock. ROESY spectra were acquired with a mixing time of 200 ms. Spectral width was 6 kHz in both direct (F2) and indirect (F1) dimensions. 2048 complex data points were collected in F2 and 512 complex data points were collected in F1 dimensions. 10 scans were taken per increment. All 1D ^1H NMR spectra were processed using NMRPIPE [29a] and NMRViewJ http://www.onemoonscientific.com/nmrview/features.html) software. Two dimensional NMR spectra were processed using XWINNMR version 3.75 (Bruker, Germany) and analyzed using SPARKY version 3.112 [29b].

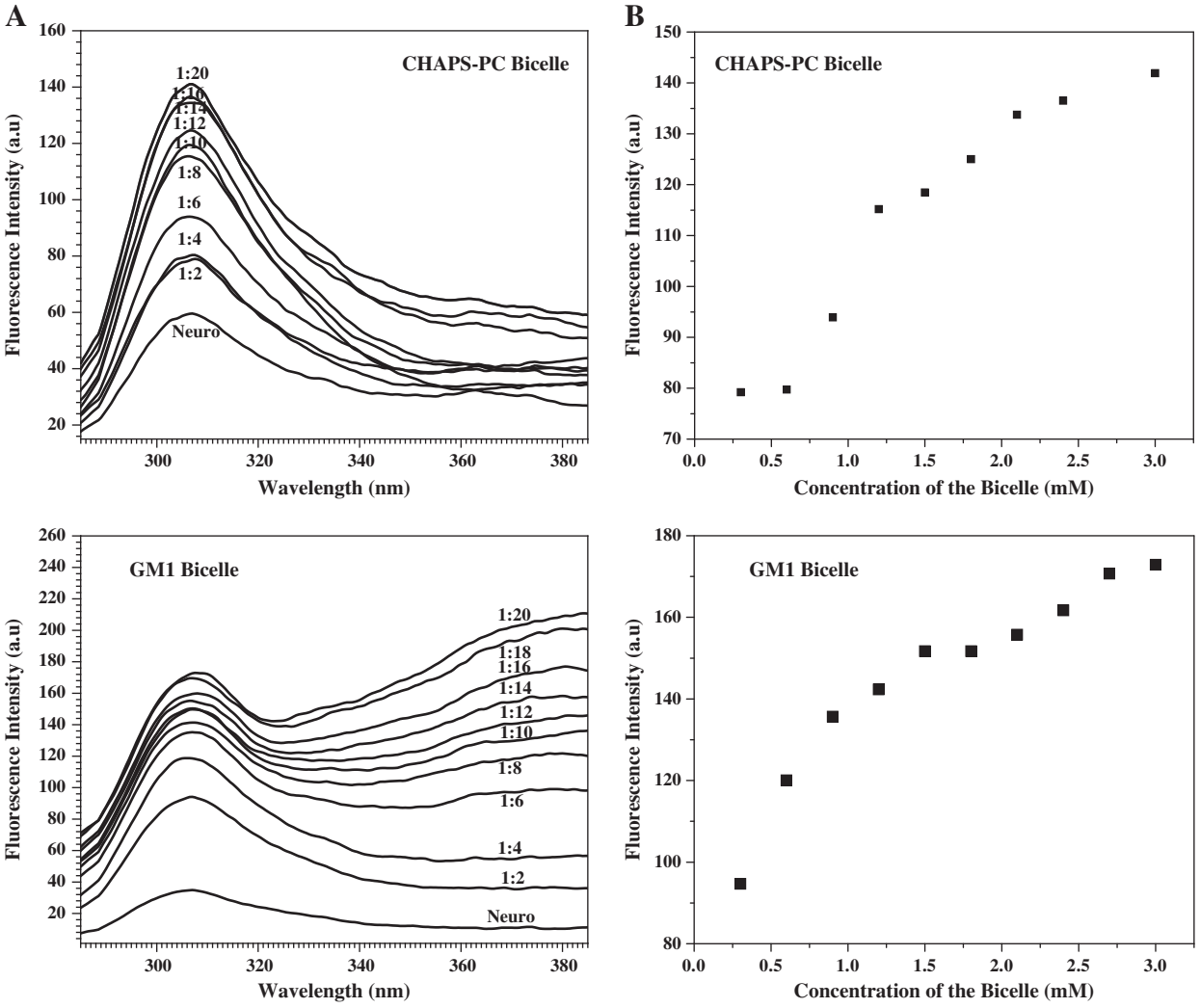

Fig. 1. A. Fluorescence titration of neurotensin with DMPC: CHAPS (1:4) bicelle, DMPC: CHAPS: GM1 (1:4:0.3) bicelle. The lower-most spectrum is of free neurotensin, and then successive spectra were obtained upon addition of bicelles to the peptide in the mole ratio shown in the figure. Fig. 1B. Plot of fluorescence intensity vs concentration of bicelle for DMPC:CHAPS(1:4) bicelle and DMPC:CHAPS:GM1(1:4:0.3) bicelle. The bicellar samples were prepared in doubled distilled H_2O of pH 5.5.

2.7. Collection and processing of diffusion NMR data

Diffusion-ordered spectroscopy (DOSY) experiments were performed on the Bruker Avance 600 MHz spectrometer. The pulse sequence used a stimulated echo with bipolar gradient pulses and two spoil gradient followed by a 3–9–19 pulse for water suppression. The gradient strength was increased from ~2% to 95% in 32 scans to attenuate the ^{1}H signal ~5% to their initial amplitude. The diffusion time Δ was 150 ms and the gradient duration δ was 5 ms. The DOSY spectra were processed using DOSYToolbox (v 0.53) [30]. Diffusion coefficient (D) was calculated by fitting the curve of signal intensity vs variable gradient strength via use of SCORE component analysis. Excluding region command was used to correct the noise and inconsistencies in the spectra which may affect a particular signal intensity. Gaussian line shape with a single exponential fit was applied to optimize the resolution of signals. The individual diffusion coefficients were calculated from DOSY using aliphatic Leu/Ile-Hδ1/Hδ2 peak resonates at 0.9 ppm for the peptide. For DMPC and CHAPS the individual diffusion coefficients were calculated from the DOSY spectra using selective acyl chain methylene proton (at 1.20 ppm) for DMPC and methylene proton (3.01 ppm at positions 25 and 3.16 ppm at position 27) for CHAPS. The average bicellar diffusion coefficient was obtained by selecting specifically the non overlapping [31] aliphatic acyl chain methylene proton of DMPC plus methylene protons of CHAPS

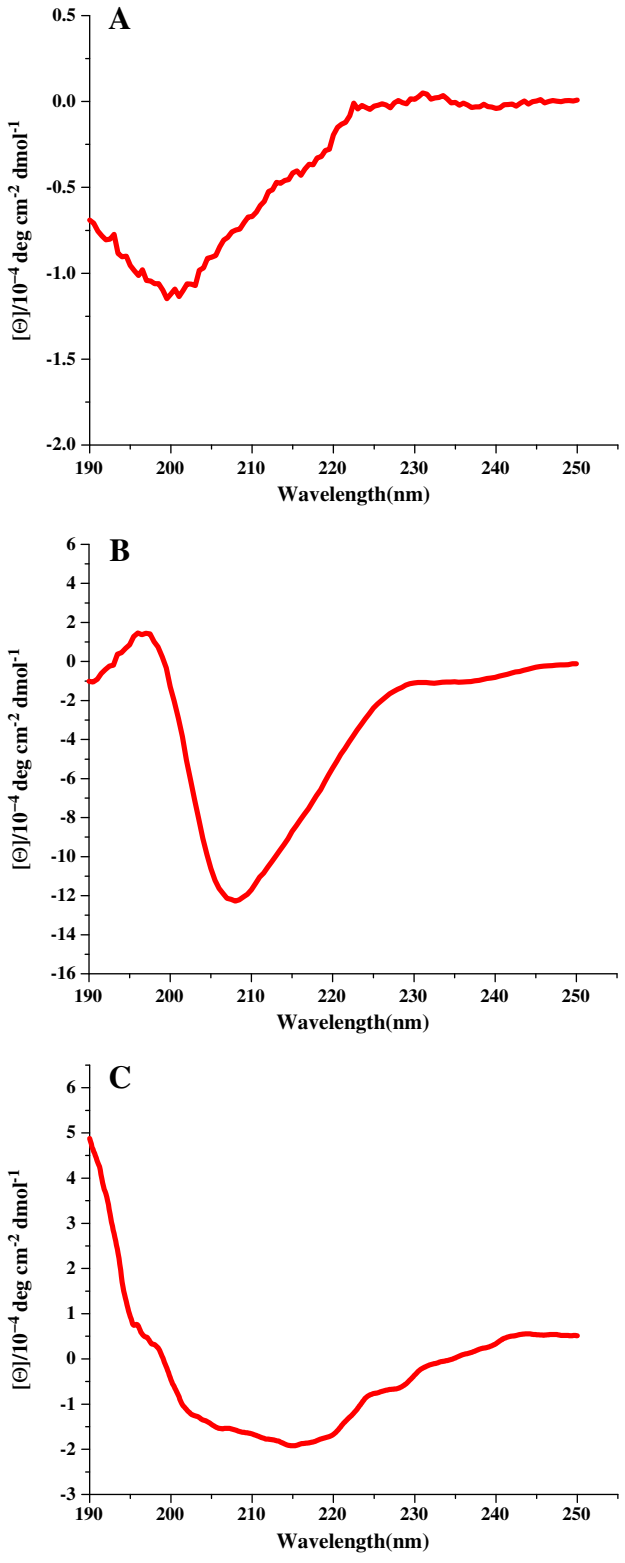

Fig. 2. Far-UV CD spectra of neurotensin 1.5 mM in water (A), in DMPC:CHAPS (1:4) bicelles (B) , in DMPC:CHAPS:GM1 (1:4:0.3) bicelles (C) at pH 5.5 and 298 K (peptide: lipid mol ratio 1:20).

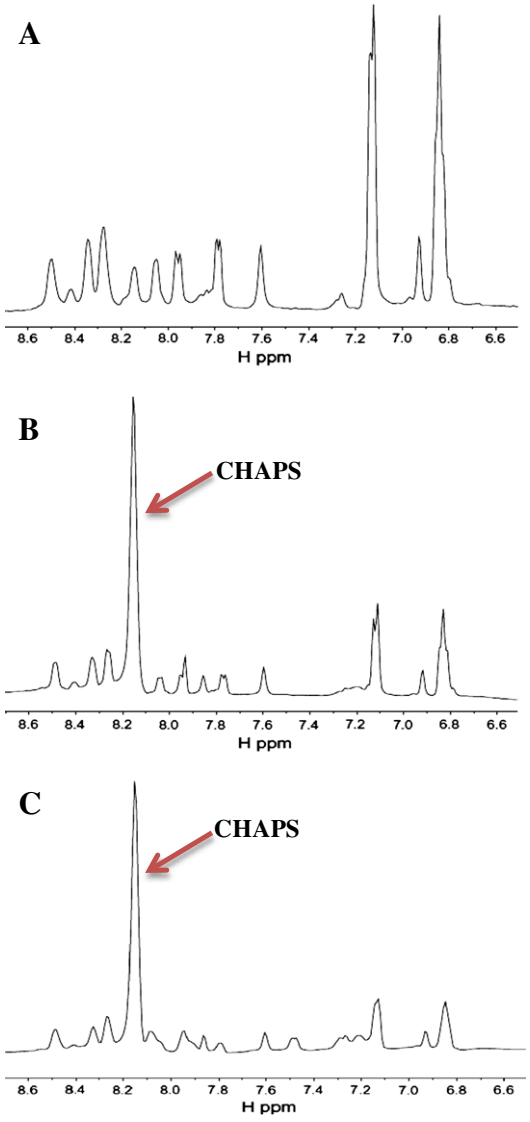

Fig. 3. 500 MHz 1-D proton NMR spectra of neurotensin (4.5 mM) in water (A), DMPC: CHAPS (1:4) bicelles (B) and DMPC: CHAPS: GM1 (1:4:0.3) bicelles (C) at pH 5.5 and 298 K (peptide: lipid 1:20 mol/mol). The spectral region indicates the fingerprint aromatic and amide region (6.5–8.6 ppm). Broadening and signal attenuation of peaks are shown from (A) to (C). Peak due to bicellar component (CHAPS proton) indicated with an arrow.

[28]. The measured diffusion coefficient (Dobs) is given by the following equation [32].

$$D_{obs} = S_{bound}.D_{bound} + S_{free}.D_{free}$$

$$D_{obs} = S_{bound}.D_{bound} + (1-S_{bound}).D_{free}$$

Where S_{free} and S_{bound} are the mol fractions of free and bound peptide, respectively. D_{free} is obtained by measuring the diffusion coefficient of peptide in water and D_{bound} corresponds to the diffusion coefficient of the bicelle. In bicellar environment, diffusion of the free peptide becomes slow due to the presence of bicelle themselves. Therefore, it is essential to correct D_{free} by introducing an obstruction factor such as:

$$D^{\phi}_{free} = D_{free}\langle A \rangle$$

Where ϕ is the volume fraction of the obstructing particles and <A> is a correction factor for spherical objects. This factor has been calculated by Gaemers and Bax for a 10% w/w bicelle solution at 20 °C assuming spherical shape of the bicelle and gave <A> = 0.95 [33]. Our bicelle can be approximated as spherical objects, thus <A> = 0.95 can be used to calculate D^{ϕ}_{free} [32].

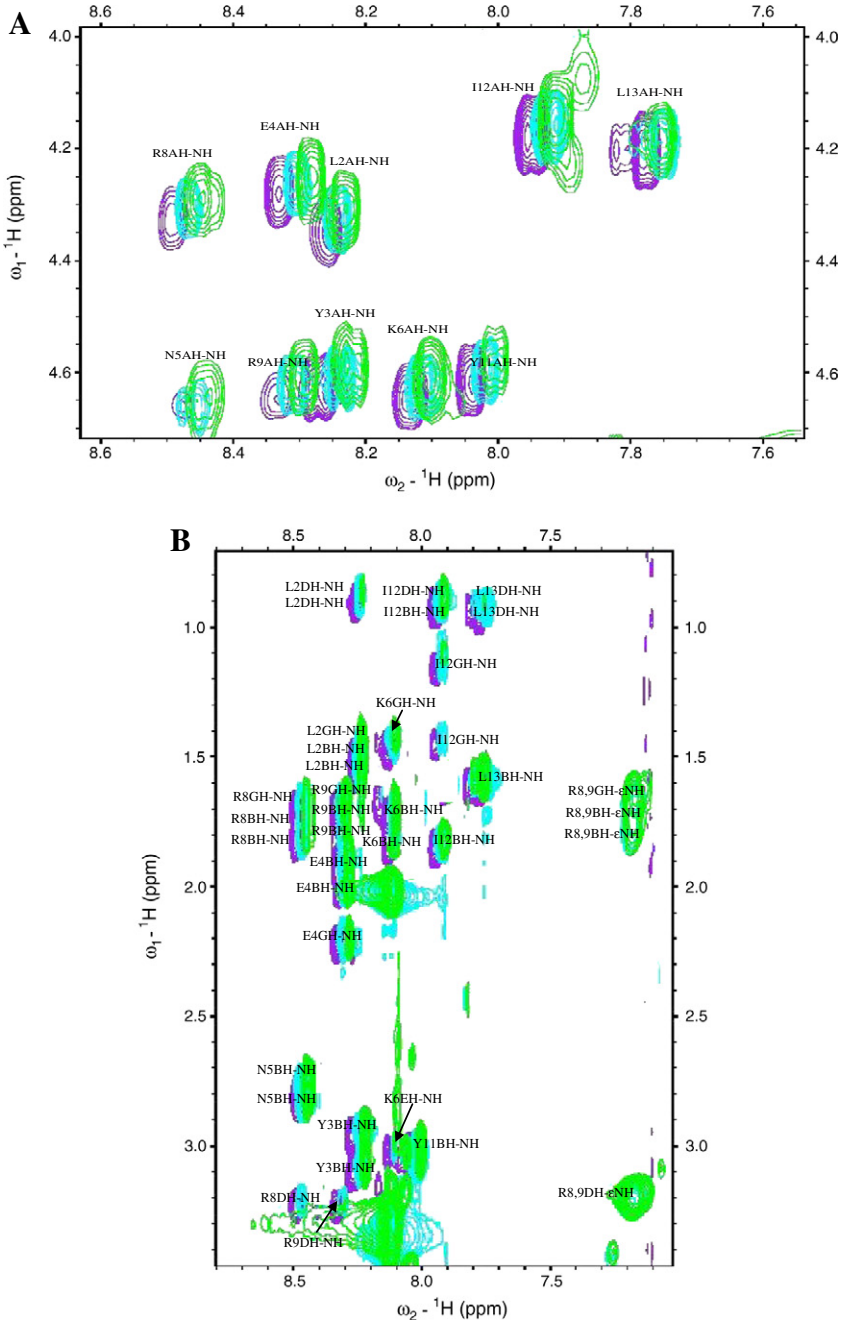

Fig. 4. A. Superimposed fingerprint region of 2D ^1H–^1H TOCSY spectra of neurotensin (4.5 mM) showing contours in water (purple) , DMPC: CHAPS (1:4) bicelles (cyan) and DMPC: CHAPS: GM1 (1:4:0.3) bicelles (green) at pH 5.5 and 298 K (peptide: lipid 1: 20 mol/mol). Fingerprint region showing alpha proton regions of TOCSY spectra A. Fingerprint region showing side chain regions of TOCSY spectra B.

3. Structure calculations

^{1}H–^{1}H ROESY cross peaks ($\tau_{mix} = 200$ ms) were assigned, integrated and then volumes were converted to distance restraints. Cross-peaks were categorized as strong, medium, weak and very weak based on their intensities. The inter proton distances (r) were derived from the ROE intensities (S) with the relation $r = c\,(S)^{-6}$, where c is a coefficient determined on the basis of ROE corresponding to a known distance. The upper distance limits were normalized against the known distance of 3.05 Å the Tyr $_{HN\text{-}H\alpha}$ for the non aromatic proton ROEs and 2.48 Å for the Tyr$_{H\delta-H\varepsilon}$ for the aromatic proton ROEs [34]. For all distance restraints the lower bound was set to 1.80 Å and the conservative upper bound were fixed respectively as 3.5, 4.0, 4.5 and 6.0 Å. The $^{3}J_{HN\text{-}H\alpha}$ coupling constants derived from the DQF-COSY spectrum were used for estimation of dihedral angles (ϕ) according to the Karplus equation: $A\cos^2\phi + B\cos\phi + C = {}^{3}J_{HN\text{-}H\alpha}$, where $A = 6.98$, $B = -1.38$ and $C = 1.72$ with $-60°$ phase difference in the dihedral ϕ. The values thus obtained were used as dihedral restraints. Dihedral angle constraints used for structure calculation have been provided in Tables S13–S15 in supporting information. Structure calculations were conducted using XPLOR-NIH software package [35]. 200 initial structures were generated from a random extended structure. The highest temperature of 3000 K was achieved during simulated annealing protocol and the final lowest temperature achieved was 12.5 K. A repel constant of 1.2 was used. High temperature dynamics stops at 10 ps or at 5000 steps. For cooling loop at each temperature 100 steps of 0.2 ps were performed. For minimization 1000 steps was used. The top 100 structures obtained from simulated annealing were further refined using the refinement protocol refine.py of XPLOR-NIH program keeping the distance and dihedral restraints on. Several rounds of structure calculations were carried out. Depending on the NOE violations, the distance constraints were adjusted in each step. From 100 structures, 40 best structures were finally selected on the basis of criteria of satisfactory covalent geometry i.e., low distance constraint violations and favorable energy values. Final 3D structures were generated using VMD-XPLOR software package version 1.5 Linux 2.4_1686 running on Linux [36]. Structural quality was evaluated using PSVS 3.1 server (psvs-1_3-dev.nesg.org/) that includes PROCHECK-NMR. Backbone and side chain hydrogen bonds were calculated using NCBS-IWS (National Centre for Biological Sciences — Integrated Web Server) (http://caps.ncbs.res.in/iws/straly.html).

4. Docking studies

Conformations of neurotensin in three environments i.e., water, CHAPS-PC bicelle and GM1 containing bicelle, were docked into the minimized Neurotensin Receptor3 (NTS3) [PDB accession code: 3F6K] structure using Autodock4 software package (http://autodock.scripps.edu). Lowest energy structures of neurotensin in water and two bicelles were pre-optimized using the autodock parameters like atom types, torsion modes and partial charges. A standard Lamarckian Genetic Algorithm was used for configurational exploration with a rapid energy evaluation using grid-based molecular affinity potentials [37]. Backbone of the peptide was kept rigid while the side chains were kept flexible during docking. Electrostatic, desolvation energies and atom type affinity grid maps on the receptor were previously calculated using auto grid. We have applied blind docking procedure and the grid was constructed covering the whole receptor. The number of grid points in the x,y,z-axis was $123 \times 123 \times 123$ with grid points separated by 0.375 Å were initially used as input. Number of runs was set as 100 for all docking. The number of energy evaluation was set to 25,000,000 and population was set to 150. The 100 independent docking poses were clustered using ADT, and the lowest energy-docking pose from the cluster was recorded. The best pose was selected depending on the lowest binding energy criteria. Modeling of the figures showing the interactions at the binding site of the ligand as well as hydrogen bonds within ligand and receptor residues were calculated using Auto Dock Tools (ADT).

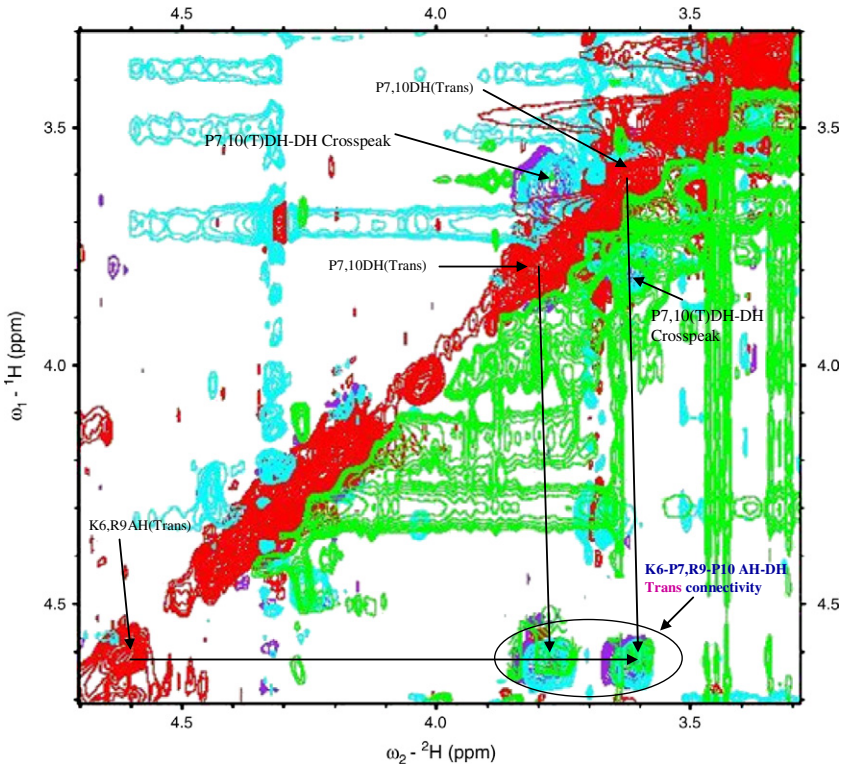

Fig. 5. Superimposed fingerprint region of 2D ^{1}H–^{1}H ROESY spectra of neurotensin (4.5 mM) showing contours in water (purple) , DMPC:CHAPS(1:4) bicelles (cyan) and DMPC: CHAPS:GM1(1:4:0.3) bicelles (green) at pH 5.5 and 298 K (peptide: lipid 1:20 mol/mol). Fingerprint region showing the trans cross peak of prolines with their preceding residues.

5. Accession codes

Distance constraints, dihedral constraints and ensemble of 40 NMR structures for neurotensin in water, DMPC: CHAPS (1:4) and DMPC: CHAPS: GM1 (1:4:0.3) bicelle have been deposited with the SMSDep bank under IDs 2lne, 2lnf and 2lng.

The assignments for neurotensin in water, DMPC: CHAPS (1:4) and DMPC: CHAPS: GM1 (1:4:0.3) bicelle have been deposited with the BioMagResBank (www.bmrb.wisc.edu) under IDs 18162, 18163, 18164 respectively.

Docked NT-NTS3 complexes (using Autodock4) of neurotensin model in water, DMPC/CHAPS (1:4) and DMPC/CHAPS/GM1 (1:4:0.3) bicelle have been deposited to PMDB under accession code: PM0077936, PM0077939 and PM0077940.

6. Results

6.1. Fluorescence spectroscopy

Fluorescence spectra of neurotensin in presence of bicelles were recorded and fluorescence titration results are depicted in Fig. 1a. Before addition of bicelles, fluorescence emission spectra of neurotensin show the peak of only tyrosine. With addition of increasing amount of CHAPS-PC bicelle in the solution fluorescence intensity gradually increases [Fig. 1a.A] indicating peptide insertion into the hydrophobic core of the membrane. This effect is more pronounced in the presence of GM1 containing bicelle [Fig. 1a.B].

6.2. Circular dichroism spectroscopy

CD experiment provides the idea about the secondary structure of the peptide induced by its surrounding environments. CD spectra were recorded for neurotensin in water, neutral DMPC: CHAPS bicelle and anionic DMPC: CHAPS: GM1 bicelle and the results are given in Fig. 2 [A,B,C]. Fig. 2A shows an intense negative minimum around 200 nm for neurotensin in water indicative of unstructured peptide [38]. In the presence of DMPC: CHAPS bicelle [Fig. 2B] neurotensin adopt 3_{10} helical structure as is evident from the intense negative minima around 208 nm [39]. In the presence of GM1 containing bicelle broad minima from 202 nm to 220 nm was observed [Fig. 2C] indicating predominating 3_{10} helical structure along with lower proportion of α-helical structure [40].

6.3. NMR studies in water and bicelles — assignments and constraints

The complete sequence-specific assignment of NT protons in water, CHAPS-PC bicelle and GM1 containing bicelle was carried out and the chemical shifts in water and bicellar medium are given in Table S1 [supporting information]. Significant line broadening occurs in the 1D proton NMR spectra in bicelle [Fig. 3B and C in comparison to Fig. 3A], suggesting that the peptide is not well exposed to water but it is partially

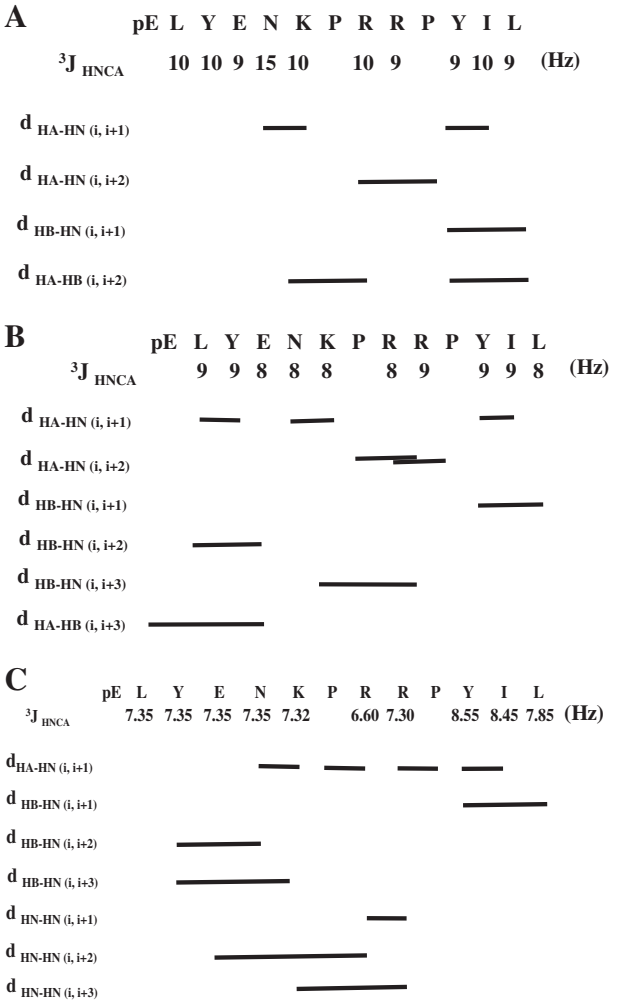

Fig. 6. Coupling constants(in Hz) and ROE connectivity plots for sequence of neurotensin (4.5 mM) in water (A), DMPC:CHAPS(1:4) bicelles (B) and DMPC: CHAPS: GM1(1:4:0.3) bicelles (C) at pH 5.5 and 298 K (peptide: lipid 1:20 mol/mol).

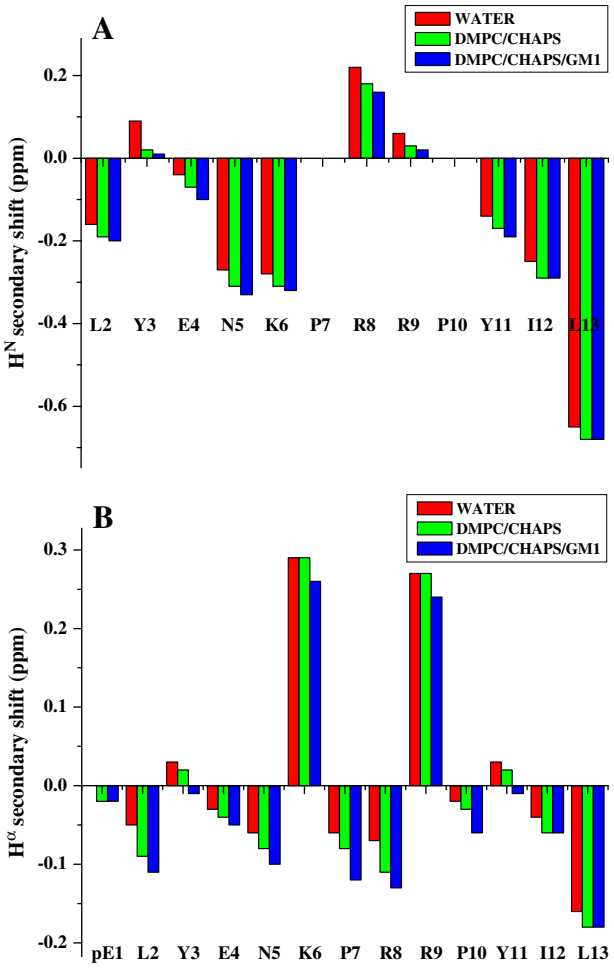

Fig. 7. Comparative amide proton (A) and alpha proton (B) chemical shift of neurotensin in water, DMPC: CHAPS (1:4) and DMPC: CHAPS: GM1 (1: 4: 0.3) bicelles at pH 5.5 and 298 K (peptide: lipid 1: 20 mol/mol). Color of the bars is labeled in the figure.

buried into the bicelle. In going from water to bicellar medium considerable amount of up field shift occur and the spectra of NT in presence of bicelle differed greatly from the spectra of neurotensin in water. The shifts in peak positions are depicted in Fig. 4a and b (^{1}H–^{1}H TOCSY). Both prolines were found in the trans-configuration as determined from the ROESY $H_{\alpha\delta}$ (i, i + 1) cross peak between each proline residue and the preceding residue [Fig. 5].

ROE connectivity [Fig. 6A,B and C] shows, $d_{NN}(i, i+1)$, $d_{NN}(i, i+2)$, $d_{\alpha N}(i, i+1)$, $d_{\alpha N}(i, i+2)$, $d_{\beta N}(i, i+1)$, $d_{\beta N}(i, i+2)$, $d_{\beta N}(i, i+3)$,$d_{\alpha\beta}(i, i+3)$, $d_{NN}(i, i+3)$, a large number of short and medium range ROEs along the entire peptide chain. Most of the measurable coupling constants [enlisted in top panel of Fig. 6A, B and C] of neurotensin in water are in the range of 9–10 Hz, in CHAPS-PC Bicelle within 8–9 Hz and ~6–8 Hz in the presence of GM1 containing bicelle. H^N secondary chemical shifts provide information about the environment of the residue [41]. If the residues are in hydrophobic environment then H^N resonances shifted to higher values relative to the average while H^N resonances shifted towards lower values if the residues are in polar environment [41]. Our result shows that H^N resonances [Fig. 7] from residue Glu4 to Lys6 differ from the rest of the peptide, indicating that this part of the peptide is involved in interaction with the hydrophobic interior of the bicelle.

6.4. Solution structure of neurotensin in water and bicelles

Distance constrains from ROESY peaks and dihedral constrains from $^3J_{HN\text{-}H\alpha}$ were used as input for structure generation using XPLOR-NIH software. Structure of NT in water, CHAPS-PC bicelle and GM1 containing bicelle are depicted in upper, middle and lower panel of Fig. 8 respectively as ensemble of 40 conformers and were selected on the basis of lowest energy and minimum violations in distance restrains. Statistical summary of the peptide structure in three mediums are provided in Table S2 [supporting information]. No long range ROE cross peak was observed for neurotensin in water. Although $d_{\alpha N(i,\ i+2)}$ cross peak observed over residue Arg8 to Pro10 [Fig. 6A] which is characteristic of turn structure still the peptide is predominately unstructured. This result is consistent with our CD spectroscopic result [Fig. 2A]. In water, 40 lowest energy conformers have backbone root-mean-square deviation (rmsd) of 1.7 Å and the heavy atom rmsd is 3.1 Å for the entire peptide length as determined from PROCHECK-NMR [Table S2. supporting information]. NCBS-IWS shows that Leu2, Glu4, Lys6, Arg9 and Tyr11 residues are involved in backbone H-bonding. C═O group of Leu 2, Glu4, Arg 9 residues act as accepter whereas NH of Glu4, Lys6, Tyr11 residues act as donor. No side chain hydrogen bonds were observed. In the Ramachandran plot [Fig. S3A. supporting information] 71.4% of the total residue lies in the most-favored region, 22.2% in allowed region and 6.4% in additionally allowed region. No preference exists for distribution of polar and nonpolar residues in water.

40 neurotensin conformers of lowest energy and minimum violation in CHAPS-PC bicelle have rmsd of 1.0 Å and heavy atom rmsd of 2.1 Å [Table S2. supporting information]. In DMPC: CHAPS bicelle the peptide adopt 3_{10} helical conformation. This 3_{10} helical conformation was confirmed by the presence of $d_{\alpha\beta}(i, i+3)$ and $d_{\beta N}(i, i+3)$ cross peak [Fig. 6B]. This result agrees with the conclusions drawn from CD result [Fig. 2B]. As evaluated by NCBS-IWS, C═O groups of pGlu, Leu2, Lys6, Pro10, Ile11 were found to be involved in backbone H-bonding with NH groups of Tyr3, Glu4, Arg8, Ile12/Leu13, Leu13 respectively. Side chain H-bonds were observed between OE2, C═O, OD1 groups of pGlu1, Tyr3, Asn5 respectively with NH2 group of Arg8. According to Ramachandran plot [Fig. S3B. supporting information], 73.1% of the total residues lie in the most favored region and 26.9% in the allowed region.

The entire peptide becomes ordered in GM1 containing bicelle in comparison to water and DMPC: CHAPS bicelle as is evident from backbone root mean square deviation of 0.8 Å and heavy atom rmsd of 1.8 Å for the entire peptide length [Table S2. supporting information]. ROE connectivity gives $d_{\beta N}(i, i+3)$ and $d_{NN}(i, i+3)$ cross peaks over residue Glu4 to Arg8 [Fig. 6C] which is the characteristics of 3_{10} helix. Moreover, $d_{NN}(i, i+2)$ cross peaks over this residue is indicative of α-helical conformation. This result indicates that in the presence of GM1 containing bicelle neurotensin exists in equilibrium between predominating 3_{10}-helical structure and small amount of α-helical structure. Different types of ROE suggesting that some conformational averaging occurring in the peptide. This result is consistent with CD spectropolarimetry result [Fig. 2C]. C═O group of Leu2, Tyr3, Glu4, Lys6, Pro10 were found to be involved in backbone H-bonding with HN of Glu4, Asn5, Lys6, Agr8/Agr9, Ile12 respectively. Side chain H-bond appears between OD1 group of Asn5 with NH2 group of Arg8. Another side chain H-bond is observed between NH of pGlu1 with OE1 of Glu4. 59.4% of the total residue lies in the most-favored region and 40.6% in allowed region of the Ramachandran plot [Fig. S3C, supporting information].

6.5. Analysis of translational diffusion measurements

Translational diffusion measurements are summarized in Table 1 [main text], and the DOSY spectra are depicted in Fig. S4–S8 in the supporting information. Diffusion of individual component is in agreement with data found in previous investigation [28]. Diffusion coefficient of neurotensin in water is $25\times10^{-11}\,m^2/s$ which decreases in

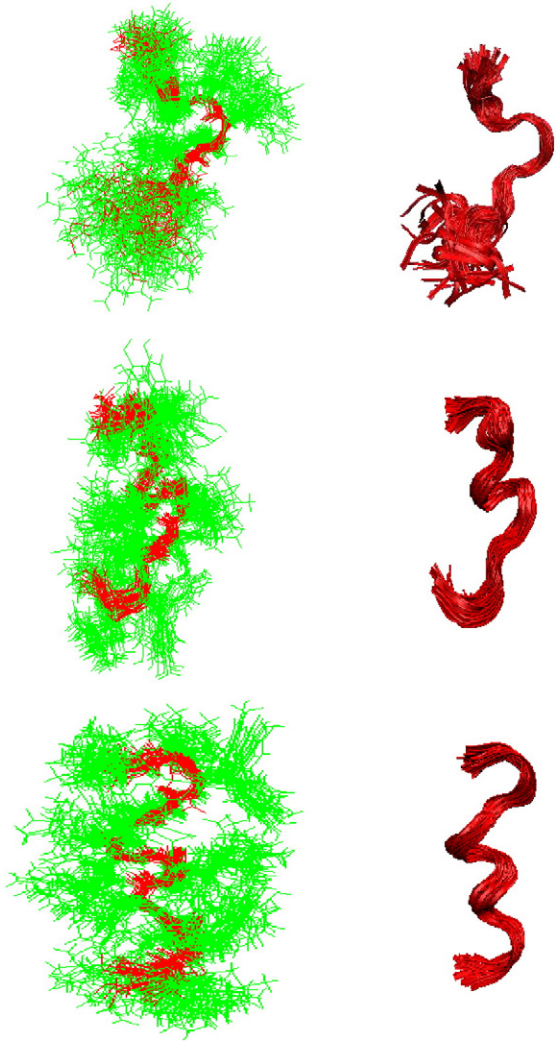

Fig. 8. Line and ribbon representations of ensemble of 40 structures of neurotensin(4.5 mM) in water (upper panel), DMPC: CHAPS(1:4) bicelles (middle panel) and DMPC: CHAPS: GM1(1:4:0.3) bicelles (bottom panel) at pH 5.5 and 298 K (peptide: lipid 1:20 mol/mol). Superimposition of ensembles of 40 conformers was done using VMD-XPLOR.

either of the bicelle [Table 1, Fig. S4]. Peptide diffusion is comparatively slower in GM1 containing bicelle than that of the CHAPS-PC bicelle [Table 1, Fig. S4]. 76% of the peptide bound to GM1 containing bicelle whereas 55% of the peptide is bound to CHAPS-PC bicelle. Based on knowledge of the % of free and bound neurotensin we have calculated comparative CSI which differs 0.01–0.03 than that of the CSI calculated from assigned chemical shift value. This does not change/alter the conclusions drawn without this minor correction. DMPC is found to diffuse slower than CHAPS probably due to the large size of DMPC and the location of DMPC being at the bicellar disc region compared to small size and the location of CHAPS at the rim [28]. Incorporation of GM1 in bicelle reduces the diffusion coefficient of only DMPC but not of CHAPS implying the presence of GM1 at the bicellar disc region [28]. Again, on addition of peptide diffusion coefficient of DMPC decreases where as diffusion coefficient of CHAPS remain unaltered [28].

7. Discussion

Neurotensin, has previously shown by others to interact with detergent micelles [10,11] and membrane mimetic solvents [10,11] resulting in only minor secondary structure changes. In the present study we have examined the interaction and structural changes of neurotensin in zwitterionic DMPC: CHAPS (1:4) and anionic DMPC: CHAPS: GM1 (1:4:0.3) bicelle. Detergent micelle has long been used as membrane mimics in spectroscopic investigation. But small size and shape of micelle influence the peptide conformation and dynamics [42]. In this context bicelle have turned out to be superior [42]. In bicelle a central planar bilayer is formed by the long-chain phospholipid surrounded by a rim of detergent or short-chain phospholipid that shields the long-chain lipid tails from water [43]. It has been reported that in small bicelle composed of DMPC and DHPC successfully solubilizes the intact outer membrane protein OmpX from *E. coli* [44]. DMPG/DMPC bicelle can deliver a functional membrane protein KCNE3 to oocyte membranes [45]. Fast tumbling isotropic ternary bicelle containing DMPC/CHAPS and ganglioside GM1 [with q = 0.25] induced specific conformation to leucine-enkephalin and substance P [27,28]. These recent reports show that bicelles have high morphological and compositional similarity with native bilayer compared to micelles which are only composed of detergents.

CHAPS are used in our study to prepare bicelle as a cholesterol-mimic. It is reported that both cholesterol and CHAPS produce similar rigidity to bicelle although former is a detergent and latter is a lipid [46]. This is due to the similarity in their molecular structure regarding the sterol region. We have recently reported [27,28] that dynamic light scattering experiments of DMPC/CHAPS and DMPC/CHAPS/GM1 bicelle show the presence of only one type of particle in solution which has size [27] much larger than CHAPS/GM1 mixed micelle size [28]. TEM have been performed with DMPC/CHAPS and DMPC/CHAPS/GM1 bicelle [27]. TEM result confirms the presence of bicellar particle with dimension < 100 nm [27]. ^{31}PNMR gives a single narrow peak for both bicelles which is the characteristics fast tumbling isotropic bicelle [27].

The preliminary idea about the interaction of the peptide with membrane was obtained from fluorescence spectroscopy [Fig. 1a]. In the presence of water NT shows the peak of tyrosine residue. After gradual addition of increasing amount of CHAPS-PC bicelle, fluorescence intensity increases [Fig.1a.A]. This effect is more pronounced in the presence of GM1 containing bicelle [Fig. 1a.B]. Hence, the interaction between NT and bicelle becomes stronger in presence of GM1. Significant increase in line broadening [11] was observed in the 1D proton NMR spectra in GM1 containing bicelle [Fig. 3C]. This is due to the increased electrostatic interaction [11] between positively charge peptide with negatively charged GM1, thus restraining the mobility [11] of the

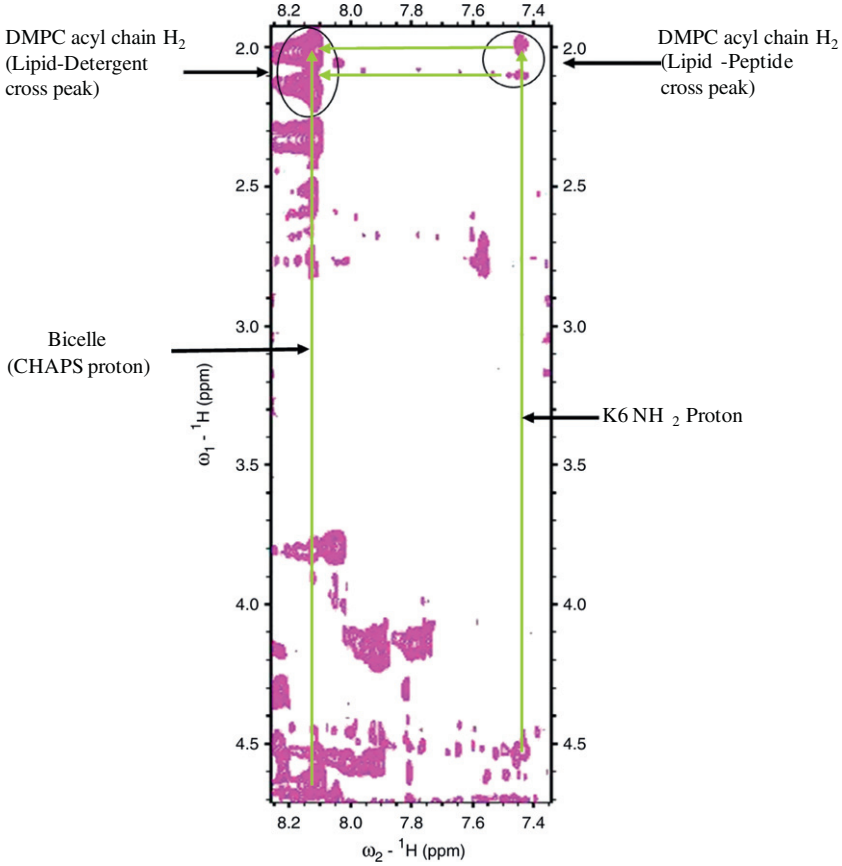

Fig. 9. 2D ^{1}H–^{1}H ROESY region showing the cross peak of neurotensin lysine side chain protons with lipid acyl chain H2 protons of DMPC in DMPC: CHAPS: GM1 bicelles (1:4:0.3) at pH 5.5 and 298 K (peptide: lipid 1:20 mol/mol).

Table 1
Measured translational diffusion coefficients of neurotensin and bicellar components DMPC and CHAPS in solution using DOSY and calculated fraction (%) of peptide bound to bicelle (pH 5.5 and 298 K).

Samples	$D_{obs} \pm 10(\times 10^{11} m^2/s)$				
	NT	DMPC	CHAPS	Bicelle	%bound
NT/water	25				
DMPC: CHAPS bicelle		10.3[a]	15.5[a]	13[a]	
NT/DMPC: CHAPS bicelle	17.2	9.25	15.6	12.9	55
DMPC:CHAPS:GM1 bicelle		9.07[b]	15.4[b]	12.3[b]	
NT/DMPC:CHAPS:GM1 bicelle	14.7	8.87	15.3	11.9	76

[a] In [DMPC]:[CHAPS] = 0.25, $D_{DMPC} = 9.38 \times 10^{11} m^2/s$, $D_{CHAPS} = 11.0 \times 10^{11}$ m^2/s and $D_{Bicelle} = 9.56 \times 10^{11}$ m^2/s (Ref. [28]).
[b] In [DMPC + GM1]:[CHAPS] = 0.25, $D_{DMPC} = 9.04 \times 10^{11} m^2/s$, $D_{CHAPS} = 10.9 \times 10^{11}$ m^2/s and $D_{Bicelle} = 9.25 \times 10^{11}$ m^2/s (Ref. [28]).

peptide and effecting the relaxation [11]. Consequently several crosspeaks arising from P7, R9 and P10 side chain protons which are very strong in the presence of CHAPS-PC bicelle, disappear [11] in the presence of ganglioside GM1 containing bicelle.

In the aromatic region of ROESY spectra of GM1 containing bicelle [Fig. 9] strongest cross peak observed between Lys NH2 group (7.45 ppm) and DMPC acyl chain H2 proton (2 ppm) which is close to ester carbonyl. This type of ROESY cross peak is absent in zwitterionic CHAPS-PC bicelle. This result demonstrates that Lys residue of neurotensin plays active role in interaction with bicelle and deeper insertion of Lys sidechain of neurotensin is achieved in GM1 containing bicelle than that of the CHAPS-PC bicelle. In GM1 containing bicelle diffusion of the peptide is slower than the CHAPS-PC bicelle [Table 1, main text] which implies that peptide partition is larger in GM1 containing bicelle than that of the CHAPS-PC bicelle. Thus, translational diffusion results confirm the effect of ganglioside GM1 on neuropeptide NT [28]. Peptide partition to the bicelle decreases the diffusion coefficient of only DMPC molecule but diffusion coefficient of CHAPS remains unaltered [Table 1, main text] [28]. This finding demonstrated that peptide preferred to reside at bicellar disk position rather than the rim.

It is possible to obtain valuable information about the peptide secondary structure from the backbone phi (ϕ) angles by measuring $^3J_{HN\text{-}HA}$ coupling constants [47]. Helical structure results if the coupling constant is in the range of 4–5 Hz [47]. The value of coupling constants [6–10 Hz] suggests that neurotensin is not fully α-helical in either water or in bicelle. The magnitudes of the coupling constants [6–8 Hz] are comparatively lowest for NT in the GM1 containing bicelle than that of water and CHAPS-PC bicelle. ROEs typical of α-helix was observed in none of the two environments i.e., in water or CHAPS-PC bicelle but in GM1 containing bicelle signature of both 3_{10} helix and α helix was observed.

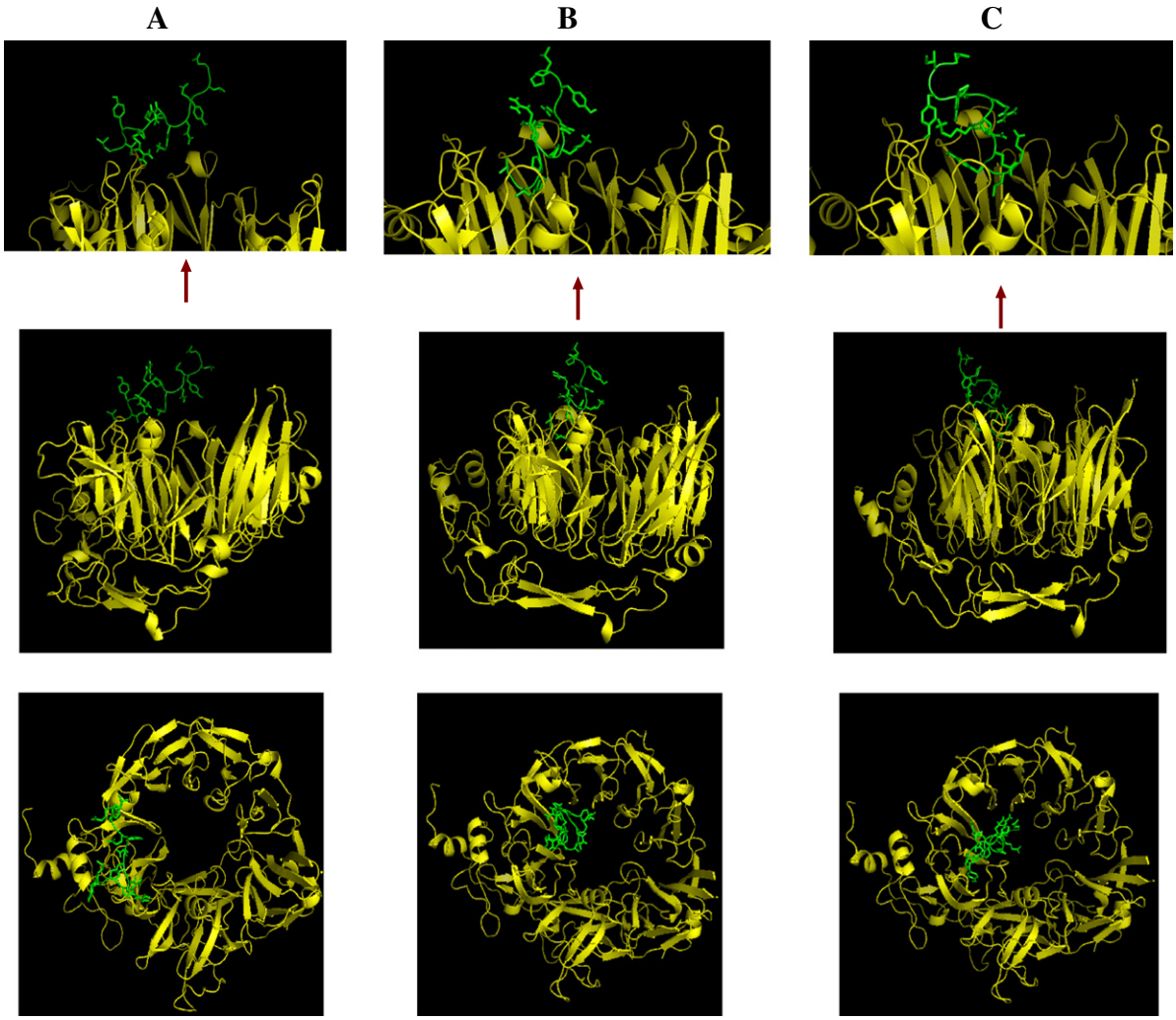

Fig. 10. Bound-state structure representation of neurotensin to its receptor NTS3 (sortilin) after docking using autodock. NTS3 is colored yellow and displaying secondary structure (middle panel). The figures in the upper panel originating from the docked complexes in middle panel indicating docking sites of neurotensin model in water (A), CHAPS-PC bicelle (B) and GM1 containing bicelle (C) respectively. The peptide neurotensin is colored green and displaying backbone cartoon presentation and side chain stick. Bottom panel representing the above plan view of the NTS3-neurotensin docking complex. Figures were generated using ADT viewer and Pymol.

Table 2
Docking result.Neurotensin/sortilin(NTS3) docking results: environments, free energies of binding, inhibition constants and proximal residues of sortilin to neurotensin.

Environments	Binding energies (kcal/mol)	Inhibition constants (μM), K_i	Interacting residues of sortilin to neurotensin
Water	−2.89	7660	Gln 255, Glu 256, Asp 278
DMPC: CHAPS	−4.96	232.16	Ser 213, Phe258, Gly303, Thr306
DMPC: CHAPS: GM1	−5.64	73.71	Glu 256, Asp278, Tyr305, Gly 307

Hence from CD [Fig. 2] and NMR [Fig. 8] it can be concluded that neurotensin is predominately unstructured in water [Fig. 2A]. In the presence of DMPC: CHAPS bicelle neurotensin adopts 3_{10} helical structures [Fig. 2B]. In the presence of GM1 containing bicelle 3_{10} helical conformation become predominating with a small amount of α-helical conformation [Fig. 2C].

To check the compatibility of neurotensin structure (obtained from NMR study) we have done *in silico* screening where representative conformer of neurotensin from each medium (obtained from NMR study) was docked on sortilin which is known as neurotensin receptor-3(NTS3). Negative value of binding free energy indicate that binding is feasible for NMR model of neurotensin in all the three environments i.e., water and bicelle [Table 2, main text]. Free energy of binding decreases considerably when the peptide conformer is changed from NMR model of neurotensin in water to either of the bicelle. Free energy of binding is lowest for neurotensin conformation in GM1 containing bicelle. Docking result [Fig.10 & Fig.S9 supporting information] suggests that neurotensin binds in the tunnel of a ten bladed β-propeller domain (residue 45-576) of the NTS3 by its C-terminal Tyr11 residue [48] (in case of neurotensin model in water the corresponding residue is Arg 9) (Fig. 10).

8. Conclusion

Considerable amounts of structural alteration occur in the inherently disordered peptide neurotensin in going from water to CHAPS-PC bicelle to GM1 containing bicelle (Fig. 11). As a whole increased stabilization of the peptide occurs in the presence of GM1 containing bicelle suggesting that interaction of neurotensin to the GM1 containing bicelle may involve conformational selection of the peptide. Our results also provide the information about the solution structure of NT in presence of membrane that is essential for its receptor recognition.

Acknowledgments

We thankfully acknowledge Bose Institute and Indian Association for the Cultivation of Science, Kolkata for the NMR experiments. We acknowledge Saha Institute of Nuclear Physics for CD spectroscopy. This work acknowledges financial support of CSIR grant CSIR-01(2400)/10/EMR-II and Nano project grant under sanction number CONV/002/NanoRAC/2008. U.L.K is thankful for CSIR fellowship under award no. 09/028(0701)/2008-EMR-I.

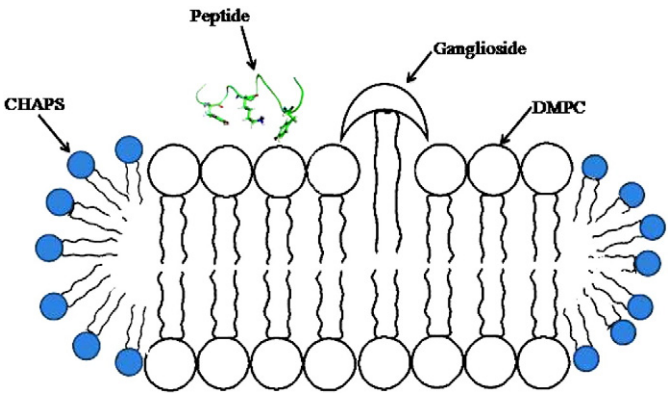

Fig. 11. Hypothesized membrane interaction of the peptide.

Appendix A. Supplementary data

Supplementary data to this article can be found online at http://dx.doi.org/10.1016/j.bpc.2012.06.003.

References

[1] E.B. Binder, B. Kinkead, M.J. Owens, C.B. Nemeroff, Neurotensin and dopamine interactions, Pharmacological Reviews 53 (2001) 453–486.
[2] R.J. Miller, D. Brown, Neurotensin, British Medical Bulletin 38 (1982) 239–245.
[3] V. Esposito, P. Girolamo, G. Gargiulo, Neurotensin-like immunoreactivity in the brain of the chicken, *Gallus domesticus*, Journal of Anatomy 191 (1997) 537–546.
[4] T. Croci, M. Landi, D. Gully, J.P. Maffrand, G.L. Fur, L. Manara, Negative modulation of nitric oxide production by neurotensin as a putative mechanism of the diuretic action of SR 48692 in rats, British Journal of Pharmacology 120 (1997) 1312–1318.
[5] P.T.F. Williamson, S. Bains, C. Chung, R. Cooke, A. Watts, Probing the environment of neurotensin whilst bound to the neurotensin receptor by solid state NMR, FEBS Letters 518 (2002) 111–115.
[6] A. Ghanizadeh, Targeting neurotensin as a potential novel approach for the treatment of autism, Journal of Neuroinflammation 58 (2010) 1–2.
[7] R.E. Carraway, A.M. Plona, Involvement of neurotensin in cancer growth: evidence, mechanisms and development of diagnostic tools, Peptides 27 (2006) 2445–2460.
[8] D. Pelaprat, Interactions between neurotensin receptors and G proteins, Peptides 27 (2006) 2476–2487.
[9] M.C. Herzig, W.G. Chapman, A. Sheridan, J.B. Rake, J.M. Woynarowski, Neurotensin receptor-mediated inhibition of pancreatic cancer cell growth by the neurotensin antagonist SR 48692, Anticancer Research 19 (1999) 213–219.
[10] J. Coutant, P.A. Curmi, F. Toma, J.P. Monti, NMR solution structure of neurotensin in membrane-mimetic environments: molecular basis for neurotensin receptor recognition, Biochemistry 46 (2007) 5656–5663.
[11] G.Y. Xu, C.M. Deber, Conformations of neurotensin in solution and in membrane environments studied by 2-D NMR spectroscopy, International Journal of Peptide and Protein Research 37 (1991) 528–535.
[12] G. van Echten, K. Sandhoff, Ganglioside metabolism. Enzymology, topology, and regulation, Journal of Biological Chemistry 268 (1993) 5341–5344.
[13] Y. Sugiura, S. Shimma, Y. Konishi, M.K. Yamada, M. Setou, Imaging mass spectrometry technology and application on ganglioside study; visualization of age-dependent accumulation of C20-ganglioside molecular species in the mouse hippocampus, PLoS One 3 (2008) 1–9.
[14] R.Y. Patel, P.V. Balaji, Structure and dynamics of glycosphingolipids in lipid bilayers: insights from molecular dynamics simulations, International Journal of Carbohydrate Chemistry 2011 (2011) 1–9.
[15] M. Hirai, H. Iwase, S. Arai, T. Takizawa, K. Hayashi, Interaction of gangliosides with proteins depending on oligosaccharide chain and protein surface modification, Biophysical Journal 74 (1998) 1380–1387.
[16] A. d'Azzo, A. Tessitore, R. Sano, Gangliosides as apoptotic signals in ER stress response, Cell Death and Differentiation 13 (2006) 404–414.
[17] M. Rochus, G. Kayser, M. Deleers, J.M. Ruysschaert, Specific interaction between soybean agglutinin and lipid bilayers containing the GM 1 ganglioside, Experientia 38 (1982) 1351–1352.
[18] K.M. Walton, K. Sandberg, T.B. Rogers, R.L. Schnaar, Complex ganglioside expression and tetanus toxin binding by PC12 pheochromocytoma cells, Journal of Biological Chemistry 263 (1988) 2055–2063.
[19] B. Tsai, J.M. Gilbert, T. Stehle, W. Lencer, T.L. Benjamin, T.A. Rapoport, Gangliosides are receptors for murine polyoma virus and SV40, EMBO Journal 22 (2003) 4346–4355.
[20] R.L. Schnaar, Glycolipid-mediated cell–cell recognition in inflammation and nerve regeneration, Archives of Biochemistry and Biophysics 426 (2004) 163–172.
[21] A. Prinetti, K. Iwabuchi, S. Hakomori, Glycosphingolipid-enriched signaling domain in mouse neuroblastoma Neuro2a cells. Mechanism of ganglioside-dependent neuritogenesis, Journal of Biological Chemistry 274 (1999) 20916–20924.
[22] T. Ariga, M.P. McDonald, R.K. Yu, Role of ganglioside metabolism in the pathogenesis of Alzheimer's disease—a review, Journal of Lipid Research 49 (2008) 1157–1175.
[23] J.S. Schneider, S. Sendek, C. Daskalakis, F. Cambi, GM1 ganglioside in Parkinson's disease: results of a five year open study, Journal of the Neurological Sciences 292 (2010) 45–51.
[24] V. Maglione, P. Marchi, A.D. Pardo, S. Lingrell, M. Horkey, E. Tidmarsh, S. Sipione, Impaired ganglioside metabolism in Huntington's disease and neuroprotective role of GM1, Journal of Neuroscience 30 (2010) 4072–4080.

[25] W. Deng, R. Li, S. Ladisch, Influence of cellular ganglioside depletion on tumor formation, Journal of the National Cancer Institute 92 (2000) 912–917.
[26] C. Chatterjee, C. Mukhopadhyay, Melittin–GM1 interaction: a model for a side-by side complex, Biochemical and Biophysical Research Communications 292 (2002) 579–585.
[27] A. Gayen, C. Mukhopadhyay, Evidence for effect of GM1 on opioid peptide conformation: NMR study on leucine enkephalin in ganglioside-containing isotropic phospholipid bicelles, Langmuir 24 (2008) 5422–5432.
[28] A. Gayen, S.K. Goswami, C. Mukhopadhyay, NMR evidence of GM1-induced conformational change of Substance P using isotropic bicelles, Biochimica et Biophysica Acta 2011 (1808) 127–139.
[29] a F. Delaglio, S. Grzesiek, G.W. Vuister, G. Zhu, J. Pfeifer, A. Bax, NMRPipe: a multidimensional spectral processing system based on UNIX pipes, Journal of Biomolecular NMR 6 (1995) 277–293;
b T.D. Goddard, D.G. Kneller, SPARKY 3, University of California, San Francisco, http://www.csb.yale.edu/userguides/datamanip/sparky/sparky_descrip.html.
[30] M. Nilsson, The DOSY Toolbox: A new tool for processing PFG NMR diffusion data, Journal of Magnetic Resonance 200 (2009) 296–302.
[31] J.F. Wang, J.R. Schnell, J.J. Chou, Amantadine partition and localization in phospholipid membrane: a solution NMR study, Biochemical and Biophysical Research Communications 324 (2004) 212–217.
[32] I. Marcotte, F. Separovic, M. Auger, S.M. Gagné, A Multidimensional ^{1}H NMR Investigation of the Conformation of Methionine-Enkephalin in Fast-Tumbling Bicelles, Biophysical Journal 86 (2004) 1587–1600.
[33] S. Gaemers, A. Bax, Morphology of three lyotropic liquid crystalline biological NMR media studied by translational diffusion anisotropy, Journal of the American Chemical Society 123 (2001) 12343–12352.
[34] T.A. Almeida, J. Rojo, P.M. Nieto, F.M. Pinto, M. Hernandez, J.D. Martin, M.L. Candenas, Tachykinins and tachykinin receptors: structure and activity relationships, Current Medicinal Chemistry 11 (2004) 2045–2081.
[35] D. Schwieters, J.J. Kuszewski, G.M. Clore, Using Xplor-NIH for NMR molecular structure determination, Progress in Nuclear Magnetic Resonance Spectroscopy 48 (2006) 47–62.
[36] D. Schwieters, G.M. Clore, The VMD-XPLOR visualization package for NMR structure refinement, Journal of Magnetic Resonance 149 (2001) 239–244.
[37] T. Hiramoto, Y. Nonaka, K. Inoue, T. Yamamoto, M. Omatsu-Kanbe, H. Matsuura, K. Gohda, N. Fujita, Identification of endogenous surrogate ligands for human P2Y receptors through an in silico search, Journal of Pharmacological Sciences 95 (2004) 81–93.
[38] M.G. Hinds, C. Smits, R. Fredericks-Short, J.M. Risk, M. Bailey, D.C.S. Huang, C.L. Day, Bim, Bad and Bmf: intrinsically unstructured BH3-only proteins that undergo a localized conformational change upon binding to prosurvival Bcl-2 targets, Cell Death and Differentiation 14 (2007) 128–136.
[39] Z. Biron, S. Khare, A.O. Samson, Y. Hayek, F. Naider, J. Anglister, A monomeric 3_{10}-helix is formed in water by a 13-residue peptide representing the neutralizing determinant of HIV-1 on gp41, Biochemistry 41 (2002) 12687–12696.
[40] N.D. Lazo, D.T. Downing, A mixture of a-helical and 310-helical conformations for involucrin in the human epidermal corneocyte envelope provides a scaffold for the attachment of both lipids and proteins, Journal of Biological Chemistry 274 (1999) 37340–37344.
[41] J. Lind, A. Graslund, L. Maler, Membrane interactions of dynorphins, Biochemistry 45 (2006) 15931–15940.
[42] A. Andersson, J. Almqvist, F. Hagn, L. Maler, Diffusion and dynamics of penetratin in different membrane mimicking media, Biochimica et Biophysica Acta 1661 (2004) 18–25.
[43] J.A. Whiles, R. Deems, R.R. Vold, E.A. Dennis, Bicelles in structure–function studies of membrane-associated proteins, Bioorganic Chemistry 30 (2002) 431–442.
[44] C. Kang, C.G. Vanoye, R.C. Welch, W.D. Van Horn, C.R. Sanders, Functional delivery of a membrane protein into oocyte membranes using bicelles, Biochemistry 49 (2010) 653–655.
[45] D. Lee, K.F.A. Walter, A.K. Bruckner, C. Hilty, S. Becker, C. Griesinger, Bilayer in small bicelles revealed by lipid−protein interactions using NMR spectroscopy, Journal of the American Chemical Society 130 (2008) 13822–13823.
[46] A. Andersson, H. Biverståhl, J. Nordin, J. Danielsson, E. Lindahl, L. Mäler, The membrane-induced structure of melittin is correlated with the fluidity of the lipids, Biochimica et Biophysica Acta 1768 (2007) 115–121.
[47] I.R. Chandrashekar, S.M. Cowsik, Three-dimensional structure of the mammalian tachykinin peptide neurokinin A bound to lipid micelles, Biophysical Journal 85 (2003) 4002–4011.
[48] E.M. Quistgaard, P. Madsen, M.K. Grøftehauge, P. Nissen, C.M. Petersen, S.S. Thirup, Ligands bind to sortilin in the tunnel of a ten-bladed β-propeller domain, Nature Structural & Molecular Biology 16 (2009) 96–98.